Marine Pollution Bulletin 62 (2011) 2496–2506

Contents lists available at SciVerse ScienceDirect

Marine Pollution Bulletin

journal homepage: www.elsevier.com/locate/marpolbul

Habitat associations of floating debris and marine birds in the North East Pacific Ocean at coarse and meso spatial scales

Andrew J. Titmus *, K. David Hyrenbach

Hawaii Pacific University, Marine Science, 41-202 Kalanianaole Hwy, Waimanalo, HI 96795, USA

ARTICLE INFO

Keywords:
Marine debris
Seabirds
Visual surveys
Spatial distribution
Subtropical gyre
Pacific Ocean

ABSTRACT

While many surface foraging seabirds ingest plastic, the spatial overlap of these far-ranging predators with debris aggregations at-sea is poorly understood. We surveyed concurrent distributions of marine birds and debris along a 4400 km cruise track within a debris accumulation area in the North East Pacific Ocean using line and strip transect methods. Analysis of debris and bird distributions revealed associations with oceanographic and weather variables at two spatial scales: daily surveys and hourly transects. Hourly bird abundance (densities; 0–9 birds km^{-2}) was higher in lower wind and shallower water. Hourly debris abundance (densities; 0–15,222 pieces km^{-2}) was higher in lower wind, higher sea-level atmospheric pressure and deeper water. These results suggest that debris and seabird abundance and community structure are influenced by similar environmental processes, but in opposing ways, with only three far-ranging seabird species (Black-footed Albatross, Cook's Petrel and Red-tailed Tropicbird) overlapping with high debris concentrations over meso-scales.

1. Introduction

The increasing abundance of marine debris in the world's oceans represents widespread and pervasive threats for wildlife via entanglement and ingestion (Laist, 1987, 1997). Plastics, in particular, have become the dominant constituent of floating debris at sea, comprising 60–80% of all marine debris worldwide (Derraik, 2002; UNEP, 2005). Because plastics are durable and inexpensive to produce, they are widely used for a variety of consumer products, many of which are single use (Laist, 1987; Moore, 2008). Moreover, their buoyant nature and longevity makes them subject to being transported and concentrated by ocean currents once they enter the marine environment (Moore, 2003). While plastics are highly resistant to aging and degradation, exposure to ultraviolet rays and seawater make the plastic polymers brittle and cause them to break into smaller fragments (Moore, 2008). The time required to biodegrade these polymers is yet unknown, especially if fragments are ingested by organisms (Andrady, 2005).

Traditionally, marine debris has been surveyed using three approaches: (i) beach surveys, (ii) at-sea net tows, and (iii) seabird stomach contents (Ryan et al., 2009). Ongoing monitoring programs have revealed increasing amounts of marine debris washed on shorelines throughout the world's coasts, from tropical shores in Hawaii and Brazil to remote sub-Antarctic islands (Barnes et al., 2009; Ryan et al., 2009). Large plastic accumulations have also been documented at-sea, both in the North Pacific (Day and Shaw, 1987; Moore et al., 2001) and the North Atlantic (Morét-Ferguson et al., 2010; Law et al., 2010).

Plastic ingestion by marine wildlife is another pervasive and increasing concern (Laist, 1987, 1997). Many seabird species in particular, are affected across the globe, from the tropics to the arctic and the Antarctic (Ryan and Fraser, 1988; Robards et al., 1995; Spear et al., 1995; Mallory, 2008). Currently, 44% of all seabird species have been confirmed to ingest plastic (Laist, 1997), underscoring the vast scale of the phenomenon. Seabirds are especially susceptible to plastic ingestion because they forage over vast oceanic ranges, and occupy a high trophic level position in marine food webs. Thus, these far-ranging marine predators collect widely dispersed plastic directly, or bioaccumulate this material through secondary ingestion via their prey (Ryan and Fraser, 1988; Spear et al., 1995; Boerger et al., 2010).

To date most studies of marine debris at sea have focused on describing the micro (<2 mm) and meso (2–20 mm) debris field (Ryan et al., 2009) by using neuston nets to sample floating material (e.g., Moore et al., 2001; Law et al. 2010). While this method accurately quantifies all of the floating debris present over the small area the net samples (0.9–1.8 km long deployment, by 1–3 m wide net opening), net tows are time intensive and provide data at coarse spatial resolution (tows separated by 10–100s km). While quantitative visual observations of debris have not been extensively conducted in the past (but see Dahlberg and Day, 1985), they provide a continuous record of the macro (20–100 mm) and mega (>100 mm) debris that can be resolved and

* Corresponding author. Address: Pelagic Ecology Lab, Hawaii Pacific University, Oceanic Institute, 41-202 Kalanianaole Hwy, Waimanalo, HI 96795, USA. Tel.: +1 808 351 2899.

E-mail address: ajtitmus@gmail.com (A.J. Titmus).

0025-326X/$ - see front matter © 2011 Elsevier Ltd. All rights reserved.
doi:10.1016/j.marpolbul.2011.08.007

analyzed to multiple spatial scales. In addition, because visual observations can be easily conducted from ships of opportunity, they provide a useful and inexpensive tool for monitoring marine debris accumulation and distribution at sea. However, visual observations are constrained by two main limitations: the inability to detect the smaller fragments (<20 mm), and the inability to retrieve the material for subsequent analysis on-board the vessel. Thus, observers have to estimate the size and color of the material in the field, during varying weather and light conditions.

This study focuses on the distribution and abundance of floating plastic and seabirds within the North Pacific Subtropical Gyre stretching between Hawaii and North America (Moore et al., 2001; Pichel et al., 2007). This region has been termed the 'Eastern Garbage Patch' due to the accumulation of large amounts of marine debris (Moore, 2003; Young et al., 2009). The objectives of this study were to: (1) quantify the amount and types of marine debris present over a large heterogeneous seascape, (2) characterize the seabird community over this same extent, and (3) assess the spatial overlap of the birds and the debris by identifying the oceanographic and weather variables which influence their concurrent distributions. To quantify the biological and physical variables which drive marine debris and seabird distributions we considered two spatial scales of analysis: smaller coarse scale (10s km) patterns which explain species level relationships in abundance and associations with physical features, and coarse-small meso scale (50–100s km) patterns which explain community-level changes in biogeographic structure (Haury et al., 1978; Hunt et al., 1999; Fauchald et al., 2000).

2. Methods

2.1. Survey area

We conducted surveys during a 20 day (2–21 August 2009) 4400 km SEAPLEX cruise aboard the *R/V New Horizon*. The aim of the cruise was to seek out and sample marine debris accumulations within the North Pacific Subtropical Gyre. To this end, the vessel left from San Diego, CA (32°42′N; 117°09′W), traveled west, reaching a maximum westerly extent of 141°W, and headed north east to Newport, OR (44°36′N; 124°3′W) (Fig. 1).

2.2. Environmental data

We collected environmental data along the length of the cruise to identify those oceanographic features and weather conditions that influence the concurrent distributions of birds and debris. To characterize the habitats of marine birds and debris, we related their sightings from the visual surveys to five environmental variables sampled every 15 s from the vessel's underway data logging system: sea surface temperature (SST), chlorophyll-a concentration (CHL), wind speed (WSP) and sea-level atmospheric pressure (SLP). We derived depth (DPT) from the National Geophysical Data Center NOAA ETOPO1, one arc-minute resolution global relief model of ocean bathymetry (Amante and Eakins, 2009), available from NOAA's National Geophysical Data Center (http://www.ngdc.noaa.gov/mgg/global/global.html). We subsampled these datasets to include only one data point every two minutes during on-effort periods of visual surveys. Based on the average speed of the vessel (17.6 km h^{-1}) this sampling rate yielded a spatial resolution of ~600 m. We calculated the mean values of each variable along the survey effort and the coefficient of variation of SST and CHL to identify hydrographic fronts (Hyrenbach et al., 2006). We also included two additional weather variables known to influence the ability to detect birds at sea (Beaufort sea state and cloud cover) (Hyrenbach et al., 2007) and two locational variables (latitude, longitude) to account for onshore/offshore gradients and other spatial influences. Overall, we used 10 explanatory variables to characterize marine debris and seabird distributions.

2.3. Seabird surveys and density estimates

A single observer (AJT) surveyed seabirds from the flying bridge of the *R/V New Horizon*, at a 10 m eye height above sea level, while the vessel was transiting between stations. The observer surveyed on one side of the track-line, based on sighting conditions (e.g., glare and wind), and recorded all birds sighted within a 300 m range following standardized strip transect methods (Tasker et al., 1984). The observer identified the birds to the lowest possible taxonomic level, and recorded their behavior (flying, sitting, feeding, ship-following), taking care to prevent re-counting birds following the vessel. To prevent observer fatigue, survey effort was restricted to a maximum of 8 h per day, and split into approximately 1 h transects (mean length = 18.1 ± 1.3 km) spread throughout the day to maximize survey coverage. The observer recorded the Beaufort sea state (BFT, scores on a quantitative scale from 0 to 7) and cloud cover (CC, quantified as the proportion of the sky obscured by clouds ranging from 0% to 100%) at the beginning and the end of each transect (Hyrenbach et al., 2007). Potential seabird prey (flying fish and flying squid), sighted within the 300 m strip width were also recorded.

We calculated densities of seabirds and their prey (number km^{-2}) by dividing the total number of individuals sighted by the area surveyed (survey distance × 300 m strip width). Because these seabird densities include multiple behaviors and assume that all species were perfectly detectable within the 300 m strip width, they provide a metric of relative rather than absolute abundance (Tasker et al., 1984; Spear et al., 1995).

2.4. Marine debris surveys and density estimates

The same observer carried out a marine debris survey concurrently with the seabird observations. Because we had no preconceptions about the ability to sight debris at sea, we followed standardized line distance sampling to develop more accurate abundance estimates (Buckland et al., 1993; Ronconi and Burger, 2009). The observer counted all marine debris sighted out to the horizon, and recorded the perpendicular distance from the ship's track-line assigned into one of seven pre-determined distance bins: 0–10, 10–50, 50–100, 100–200, 200–300, 300–600 and >600 m. Perpendicular distance from the ship was determined using a hand-held range finder when the debris was directly abeam of the ship (Heinemann, 1981), and these distances were used to determine the effective strip width (ESW) (Buckland et al., 1993). In addition, each piece of marine debris was assigned to one of three pre-determined size classes, based on its larger dimension: small (2–10 cm), medium (10–30 cm) and large (>30 cm). The color of each piece and a description were also recorded.

Line distance sampling quantifies how the ability to sight targets depends on their distance from the trackline, as well as on both inherent qualities (e.g., target color and size) and external conditions (e.g., weather conditions). Thus, surveys and targets with varying detectability are pooled and analyzed separately (e.g., Forney and Barlow, 1993; Hyrenbach et al., 2001). In this analysis, we considered two inherent target qualities (the size and color of the marine debris) and one external factor (the sea state during surveys).

We pooled the marine debris sightings into nine groups based on size and color, to provide larger sample sizes for calculating the ESW estimates (Table 4). We considered three size classes (small, medium, large) and three color classes: white, high

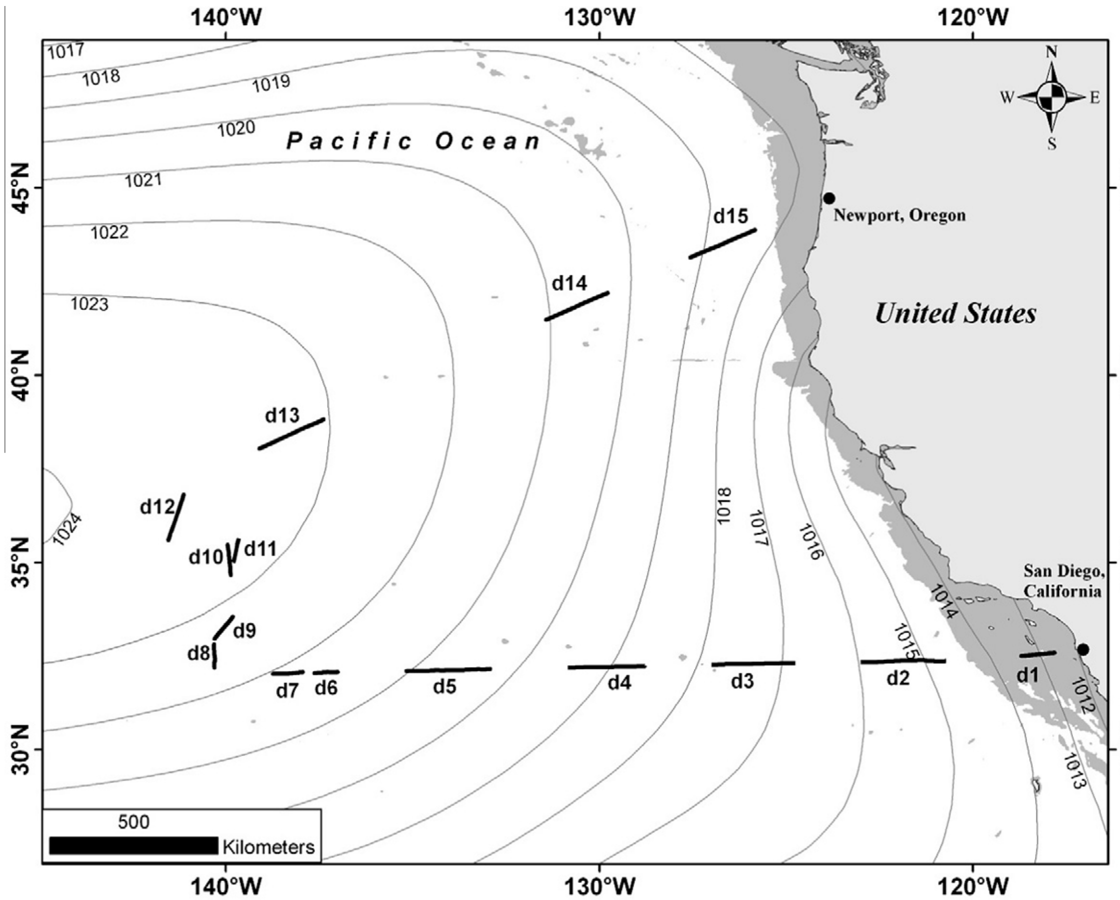

Fig. 1. Map of the North East Pacific Ocean, showing the daily survey effort (black lines). Monthly (August 2009) average sea level atmospheric pressure (mbar) contours are superimposed and depths shallower than 3000 m are shaded.

visibility colors (orange, yellow, red) and low visibility colors (green, brown, blue, black, clear). To examine the influence of sighting conditions on marine debris detectability we performed simple linear regressions of sighting distances as a function of Beaufort sea state for each debris group separately. Because there were no significant negative slopes, indicative of decreasing detectability with increasing sea state we used marine debris sightings across the entire range of environmental conditions (Beaufort range 0–4) in subsequent analyses. We used the DISTANCE 6 software (Thomas et al., 2010) to calculate the ESW's for the nine aforementioned marine debris groups.

As the passive targets were neither attracted to, nor repulsed from the vessel, we calculated the detection function $f(0)$ using half normal, hazard rate and uniform models (Hyrenbach et al., 2001). For each marine debris group, we selected the model which best described the perpendicular sighting distance distribution and minimized Akaike's Information Criteria (AIC). Next, we calculated correction factors to standardize the apparent densities of each of the nine marine debris groups with respect to the group with the widest ESW (Ballance and Pitman, 1998). The total number of sightings was multiplied by the correction factor for each group to yield a corrected number of sightings. Densities (pieces km^{-2}) for each group were determined by dividing the corrected number of sightings by the effective area surveyed (survey distance × maximum ESW).

2.5. Spatial scales of analysis

To examine the role of oceanographic processes and physical features in structuring the dispersion of marine birds and debris, we analyzed their overlap at two different spatial scales. We first used the one hour transects to determine the environmental variables influencing the small coarse scale (10s km) patterns. To avoid potential detectability biases, we discarded from the analysis those transects where the ship speed was <15 km h^{-1}. To ensure our analysis addressed a consistent spatial scale, we also removed from the dataset those transects that were anomalously long or short, and thus fell outside of the mean ± 2 SD transect distance (range = 14.9–21.1 km, n = 74 transects).

We then used daily surveys to determine the small meso scale (100s km) community composition and environmental correlates of debris and seabird species distributions across the study area. We pooled the hourly transect data into 15 daily surveys, separated by nightly transit periods (range = 33.7–152.5 km, n = 15 daily surveys).

2.6. Statistical analysis

The coarse-scale analysis (at the transect scale) investigated seabird and marine debris aggregation, by characterizing their abundance when all species (birds) and groups (marine debris) were pooled. Before we conducted the statistical analyses, we addressed the lack of normality in the seabird and marine debris densities by log transforming the data as follows: $y' = \log(y + 1)$ (Zar, 1984). We also determined to what extent the 10 explanatory variables were cross-correlated by performing pair-wise Pearson correlations (Zar, 1984).

Because many of these variables were cross-correlated, we determined the environmental variables driving seabird and marine debris distribution using forward Generalized Linear Models

(GLMs) step-wise procedures, whereby the model assesses each environmental variable and retains those with the highest explanatory power.

We adopted a hierarchical approach designed to analyze the geographic patterns first, and to characterize the associations with environmental variables next. We anticipated a geographic pattern in the distribution of marine debris and seabirds, due to the underlying distribution of marine debris (e.g., the eastern garbage patch) and seabirds (e.g., distance to shore-based breeding colonies). Thus, we first performed a best-fit step-wise GLM using only latitude (LAT) and longitude (LON). We then removed these geographic effects by performing a second GLM on the residuals from the geographic model using the remaining environmental variables.

The meso-scale analysis (at the daily survey scale) examined the distribution of individual seabird species and marine debris groups, using the 15 daily surveys. We removed those seabird species only sighted during one survey day because they did not provide information for quantifying community structure (McCune and Mefford, 1999). We averaged the environmental variables across each day, and analyzed the daily scale distribution of seabirds and marine debris using Non-metric Multi-Dimensional Scaling (NMDS). We chose NMDS, which plots the samples (daily transects) and the individual taxa (seabird species and marine debris groups) in relation to multivariate axes of environmental variables, because of its lack of assumptions about the underlying statistical distributions and its ability to organize the data along a continuum, rather than into discrete groupings (McCune and Mefford, 1999). Because the number of seabirds and debris sighted daily varied greatly, we normalized the daily surveys and weighted each daily sample equally in the NMDS analysis using the Sorensen (Bray–Curtis) similarity index (Hyrenbach et al., 2007). We used the PC ORD software to conduct these analyses, and assessed statistical significance using randomizations with 1000 iterations (McCune and Mefford, 1999).

3. Results

3.1. Oceanographic observations and environmental conditions

We surveyed a total of 1343 km along the 4400 km cruise track, during 74 hourly transects and 15 daily surveys, separated by "off effort" night-time periods. The SEAPLEX cruise traveled from the southern California Current and into the subtropical gyre, an area influenced by the North East Pacific subtropical high pressure center (Fig. 1). During the westward transit, the vessel traveled over deep water (>3000 m) and did not cross any seamounts (Fig. 2C). As we moved west, SST and SLP steadily increased (Fig. 2D and I), Wind speed was low and variable (Fig. 2F) and CHL remained consistently low (Fig. 2E). Conditions changed during the North-East transit towards the Oregon coast: the depth decreased and the SST dropped. Wind speed and SLP increased until a storm system interrupted our observations (after day 13). When surveys resumed (day 14), SLP and Wind speed had decreased considerably,

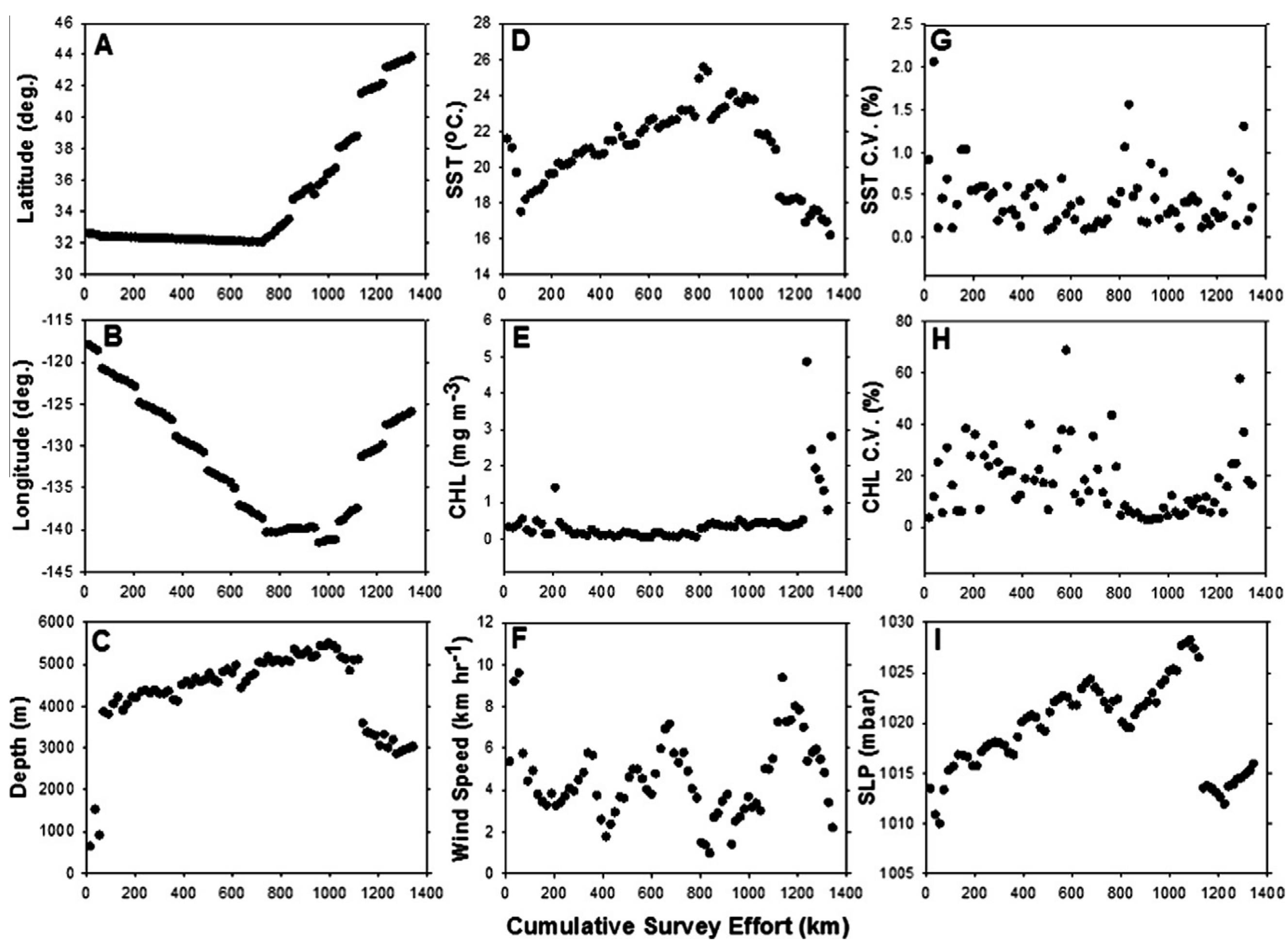

Fig. 2. Spatial distribution of mean (A) latitude, (B) longitude, (C) depth, (D) sea surface temperature (SST), (E) chlorophyll-a concentration (CHL), (F) wind speed, (G) SST coefficient of variation, (H) CHL coefficient of variation and (I) sea level pressure (SLP) for 74 one hour transects surveyed along the cruise.

and CHL reached 0.2 mg m^{-3} CHL, indicating we had crossed the Transition Zone Chlorophyll Front and entered the North Pacific Transition Zone close to the Oregon coast (Polovina et al., 2001; Chai et al., 2003).

The ten environmental and habitat variables considered were cross-correlated at the transect scale, with 25 out of 45 pair-wise comparisons yielding significant correlations. The variables were cross-correlated to a lesser degree at the daily survey scale, with 14 out of 45 pair-wise comparisons significantly correlated (Table 1). These results revealed a strong geographic effect, with both latitudinal and longitudinal gradients, and highlighted the influence of the high atmospheric pressure cell, characterized by lower wind, deeper depths, and waters of higher temperature and lower chlorophyll concentrations.

3.2. Seabird densities

We sighted 235 birds comprising 22 species over the extent of the cruise, and identified 92.7% to species (Table 2). Of these, 69% were tubenoses (order *Procellariiformes*), 26% were terns, phalaropes, skuas, gulls and alcids (order *Charadriiformes*) and 5% were tropicbirds and boobies (order *Pelecaniformes*). The avifauna changed over the cruise, and was dominated numerically by Black-footed Albatross (*Phoebastria nigripes*) and Red-tailed Tropicbird (*Phaethon rubricauda*) in the southern warm-water areas (days 5–10) and by Leach's Storm-petrel (*Oceanodroma leucorhoa*) and Sooty Shearwater (*Puffinus griseus*) in the cooler more productive waters of the CCS (days 1–4 and 11–15) (Table 3). The overall bird densities varied across transects (range = 0–9.01 birds km^{-2}) and daily surveys (range = 0.04–2.93 birds km^{-2}) (Fig. 3A, Table 3). The highest densities occurred off Oregon and within the transition zone waters, while the lowest densities occurred far from land, within the low productivity and warm gyre waters (Fig. 3A, Table 3).

3.3. Marine debris densities

We sighted a total of 3868 pieces of marine debris over the extent of the cruise, 95.5% of which were identified as plastic. The remainder was comprised of line, polystyrene foam, glass, wood, cardboard and burlap. While some intact objects were seen, fragments were the most dominant plastic (90% of total, $n = 3464$). The marine debris density was also highly variable on both the hourly transect scale, ranging from 0–15,222 pieces km^{-2}, and the daily survey scale, ranging from 0 to 6334 km^{-2}. Small pieces (2–10 cm) were the most abundant, accounting for 81% of the total, with medium (10–30 cm) and large (>30 cm) pieces accounting for 14% and 5%, respectively. Despite observing a wide range of marine debris colors, white was the dominant color with 89% of the total (Fig. 4).

The detectability of the marine debris declined as the distance from the vessel increased (Fig. 5). While large pieces were sighted out to a 600 m range, 54% occurred within the first distance bin (0–10 m) and only 1% occurred within the 300–600 m bin. In comparison, 97% of the small pieces occurred within the 10 m bin, and were only observed out to a range of 50 m. Yet, the perpendicular sighting distances for the nine marine debris groups we considered did not decrease linearly as sea state increased, as evidenced by the lack of significant negative slopes (sighting distance = intercept + (m ∗ sea state)), suggesting an absence of biases in detectability due to changing weather conditions (Grp1, $r^2 = 0.002$, $m = 3.2 \pm 8.6$, $p = 0.709$; Grp2, $r^2 = 0.140$, $m = 38.6 \pm 17.2$, $p = 0.032$; Grp3, $r^2 = 0.000$, $m = 0.4 \pm 3.5$, $p = 0.906$; Grp4, $r^2 = 0.006$, $m = -2.2 \pm 1.5$, $p = 0.155$; Grp5, $r^2 = 0.029$, m = 3.2 ± 2.3, $p = 0.154$; Grp6, $r^2 = 0.008$, $m = 4.9 \pm 5.1$, $p = 0.331$; Grp7, $r^2 = 0.017$, $m = 0.9 \pm 0.1$, $p < 0.001$; Grp8, $r^2 = 0.078$, $m = 3.1 \pm 1.6$, $p = 0.056$; Grp9, $r^2 = 0.006$, $m = 0.9 \pm 1.6$, $p = 0.556$) (Table 4).

Calculating the corrected marine debris densities required that we truncate the most distant sightings, leaving a sample size of 3715 pieces. Selecting the best fit model and truncation distance for each marine debris group resulted in effective strip width's (ESW) ranging from 33.2 m for large white pieces to 5.4 m for large low visibility pieces (Fig. 5, Table 4). Using the group-specific correction factors, we calculated a corrected number of sightings and used these corrected sightings and the maximum ESW of 33.2 m to estimate marine debris densities ranging from 1.57 pieces km^{-2} for large white pieces to 392.94 pieces km^{-2} for small white pieces (Table 5).

These correction factors were then used to calculate the corrected total marine debris densities for each hourly transect (Fig. 3B). Densities of marine debris were lowest close to the

Table 1
Cross-correlations between the environmental and habitat variables sampled during hourly transects and daily surveys. Significant correlations highlighted in bold font.

	WSP	DPT	SST	TCV	CHL	CCV	SLP	CC	LAT	LON
(A) Hourly transect scale: Pearson correlation, r critical = 0.232, n = 74										
WSP	–	**<0.05**	**<0.05**	**<0.05**	>0.1	>0.1	**<0.05**	**<0.05**	>0.1	**<0.05**
DPT	−0.479	–	**<0.05**	>0.1	0.05 < *p* < 0.1	**<0.05**	**<0.05**	>0.1	**<0.05**	>0.1
SST	−0.419	+0.877	–	>0.1	**<0.05**	**<0.05**	**<0.05**	**<0.05**	**<0.05**	**<0.05**
TCV	−0.339	−0.081	−0.007	–	>0.1	>0.1	>0.1	>0.1	>0.1	0.05 < *p* < 0.1
CHL	+0.007	−0.205	−0.347	+0.167	–	**<0.05**	**<0.05**	**<0.05**	**<0.05**	>0.1
CCV	+0.175	−0.379	−0.346	+0.095	−0.419	–	>0.1	>0.1	**<0.05**	**<0.05**
SLP	−0.294	+0.869	+0.753	−0.187	−0.285	−0.178	–	>0.1	**<0.05**	**<0.05**
CC	+0.233	−0.120	−0.298	−0.151	+0.276	+0.012	+0.042	–	**<0.05**	>0.1
LAT	+0.031	+0.391	−0.307	+0.153	+0.808	−0.340	−0.289	+0.391	–	>0.1
LON	+0.261	−0.111	−0.807	+0.203	+0.087	+0.402	−0.756	−0.111	−0.055	–
(B) Daily survey scale: Pearson correlation, r critical = 0.514, n = 15										
	WSP	DPT	SST	TCV	CHL	CCV	ATM	CC	LAT	LON
WSP	–	**<0.05**	**<0.05**	>0.1	>0.1	>0.1	>0.1	>0.1	>0.1	0.05 < *p* < 0.1
DPT	−0.669	–	**<0.05**	**<0.05**	>0.1	>0.1	**<0.05**	>0.1	>0.1	**<0.05**
SST	−0.549	+0.629	–	0.05 < *p* < 0.1	**<0.05**	**<0.05**	**<0.05**	0.05 < *p* < 0.1	0.05 < *p* < 0.1	**<0.05**
TCV	+0.141	−0.628	−0.453	–	>0.1	0.05 < *p* < 0.1	**<0.05**	>0.1	>0.1	>0.1
CHL	+0.007	−0.348	−0.571	+0.223	–	>0.1	>0.1	>0.1	**<0.05**	>0.1
CCV	+0.097	−0.142	−0.514	+0.470	+0.158	–	>0.1	>0.1	>0.1	0.05 < *p* < 0.1
ATM	−0.403	+0.842	+0.664	−0.546	−0.353	−0.293	–	>0.1	>0.1	**<0.05**
CC	+0.371	−0.056	−0.467	−0.101	+0.402	+0.013	+0.125	–	**<0.05**	>0.1
LAT	+0.171	−0.193	−0.511	−0.188	+0.744	−0.256	−0.209	+0.626	–	>0.1
LON	+0.469	−0.839	−0.750	+0.006	+0.268	+0.503	−0.824	−0.075	+0.006	–

Table 2
Summary of seabird observations over the cruise area during August 2009, showing the total and relative number of individuals and the number of days that each species was sighted (total = 15). Observations are a summary of all 83 hourly transects before removal of data for analysis purposes. Species in bold font were included in the daily scale NMDS analysis. Also included are notes on the presence (Y) or absence (N) of plastic ingestion records originating from the literature (Sileo et al., 1990; Spear et al., 1995; Imber, 1996; Robards et al., 1997; Nevins et al., 2005). Plastic ingestion for those species without published records is labeled as unknown (U).

Order	Common name	Scientific name	Total birds	Prop. (%)	Total days	Ingest plastic
Procellariiformes	**Black-footed Albatross (BFAL)**	*Phoebastria nigripes*	17	7.23	10	Y
	Ashy Storm-petrel (ASSP)	*Oceanodroma melania*	6	2.55	3	U
	Fork-tailed Storm-petrel (FTSP)	*Oceanodroma furcata*	3	1.28	1	Y
	Leach's Storm-petrel (LESP)	*Oceanodroma leucorhoa*	41	17.45	8	Y
	Least Storm-petrel (LSSP)	*Oceanodroma microsoma*	2	0.85	1	U
	Kermadec Petrel (KEPE)	*Pterodroma neglecta*	1	0.43	1	N
	Cook's Petrel (COPE)	*Pterodroma cooki*	6	2.55	3	Y
	Bulwer's Petrel (BUPE)	*Bulweria bulwerii*	2	0.85	1	N
	Buller's Shearwater (BUSH)	*Puffinus bulleri*	9	3.83	2	Y
	Sooty Shearwater (SOSH)	*Puffinus griseus*	61	25.96	1	Y
	Pink-footed Shearwater (PFSH)	*Puffinus creatopus*	1	0.43	1	Y
	Unidentified Shearwaters		8	3.40	1	
	Unidentified Petrels		1	0.43	2	
	Unidentified Storm-petrels		4	1.70	2	
Pelecaniformes	**Red-billed Tropicbird (RBTR)**	*Phaethon aethereus*	2	0.85	2	U
	Red-tailed Tropicbird (RTTR)	*Phaethon rubricauda*	7	2.98	3	U
	White-tailed Tropicbird (WTTR)	*Phaethon lepturus*	1	0.43	1	U
	Brown Booby (BRBO)	*Sula leucogaster*	1	0.43	1	N
Charadriiformes	**Red-necked Phalarope (RNPH)**	*Phalaropus lobatus*	23	9.79	2	U
	South-polar Skua (SPSK)	*Catharacta maccormicki*	2	0.85	2	U
	Pomarine Skua (POSK)	*Stercorarius pomarinus*	4	1.70	1	N
	Elegant Tern (ELTE)	*Sterna elegans*	8	3.40	1	U
	Common Tern (COTE)	*Sterna hirundo*	15	6.38	2	U
	Arctic Tern (ARTE)	*Sterna paradisaea*	1	0.43	1	U
	Rhinoceros Auklet (RHAU)	*Cerorhinca monocerata*	5	2.13	1	Y
	Unidentified Gulls		3	1.28	1	
	Unidentified Terns		1	0.43	1	
	Grand total		235	100.00		

Table 3
Survey effort and location of the daily transect surveyed along the cruise track, showing the average seabird and marine debris densities, and the relative abundance of the dominant seabird species (see Table 2 for species codes).

Day	Effort (km)	Seabird density (birds/km^2)	Dominant seabird species	Relative abundance (%)	Debris density (pieces/km^2)	Midpoint latitude	Midpoint longitude
1	55.65	1.08	ELTE	29	0.00	32.5405	−118.2930
2	152.47	0.42	LESP	53	1.76	32.3668	−121.9119
3	150.32	0.22	LESP	80	6.90	32.2923	−125.8086
4	130.30	0.23	LESP	50	45.17	32.2128	−129.8737
5	128.94	0.08	BFAL, COPE	50, 50	82.98	32.1240	−133.8613
6	56.80	0.22	BFAL	50	194.92	32.0676	−137.3432
7	57.21	0.17	BFAL	75	123.05	32.0412	−138.2546
8	55.06	0.31	RTTR	60	391.17	32.4559	−140.3073
9	52.10	0.07	SPSK	100	6334.12	33.2349	−140.0765
10	72.24	0.27	BFAL, RTTR	50, 50	475.03	35.0209	−139.8989
11	33.73	0.38	LESP	75	3892.64	35.4792	−139.6987
12	85.04	0.04	LESP	100	558.06	36.3798	−141.2742
13	89.88	0.04	LESP	100	110.90	38.4760	−138.2249
14	105.68	0.76	RNPH	67	0.00	41.8219	−130.6510
15	118.24	2.93	SOSH	53	9.94	43.4650	−126.8149

California coast and highest within the subtropical gyre. While densities declined as the vessel approached Oregon, a spike in density was observed within the transition zone. At the daily transect scale, marine debris densities ranged from 0 to 6334.12 pieces km^{-2} (Table 3). Daily density distributions mirrored those at the hourly transect scale, with the highest densities in the subtropical gyre and an area of high density within the transition zone waters off Oregon (day 15, Fig. 6B).

3.4. Transect scale communities

We used the average values of the 10 environmental and habitat variables measured within the 74 hourly transects, along with hourly transect scale densities for seabirds (all taxa combined) and marine debris (all groups combined) to identify the variables with the most explanatory power. The step-wise GLM first accounted for geographic effects, by relating seabird and debris density to latitude and longitude (Table 6A and C). We then analyzed the residuals using a second step-wise GLM with the remaining environmental variables. The GLM results showed that marine debris density was negatively related to latitude and longitude (Table 6A). Once this geographic effect was accounted for, the marine debris was positively related to depth and sea-level pressure, and negatively related to wind speed (Table 6B). Together, these analyses explained 93% of the variance in the log-transformed marine debris data. The GLM results also showed that seabird density was positively related to latitude and longitude (Table 6C). Finally, after accounting for this geographic effect, seabird density

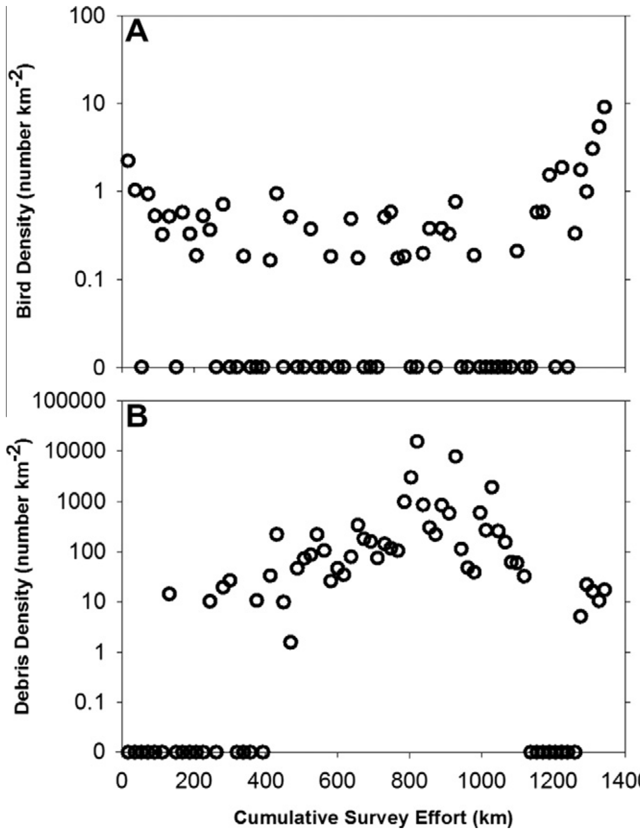

Fig. 3. Density of seabirds (A) and marine debris (B) for 74 one hour transects surveyed along the cruise.

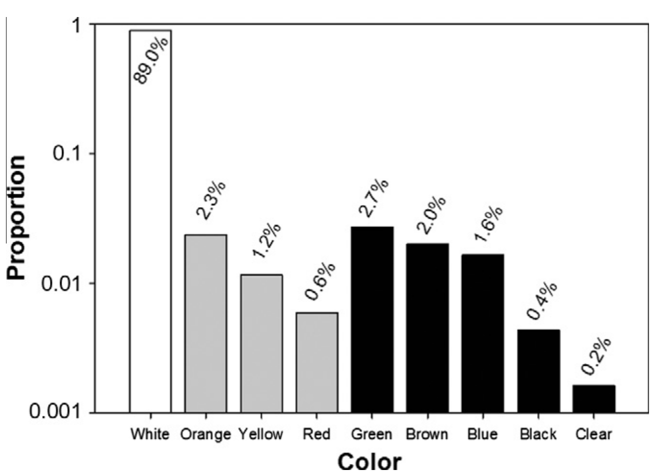

Fig. 4. Proportion of observed marine debris item colors, classified by their relative detectability. Empty bars represent the most visible color (white), gray bars denote highly visible colors and black bars represent low visibility colors.

residuals were negatively related to wind speed and depth (Table 6D). Together, these analyses explained 45% of the variance in the log-transformed seabird data. Taken together, the GLM results suggest that seabirds and marine debris are spatially separated based on water depth.

3.5. Daily scale communities

The 15 daily transects were analyzed using NMDS ordination. The number of daily marine debris observations for each group

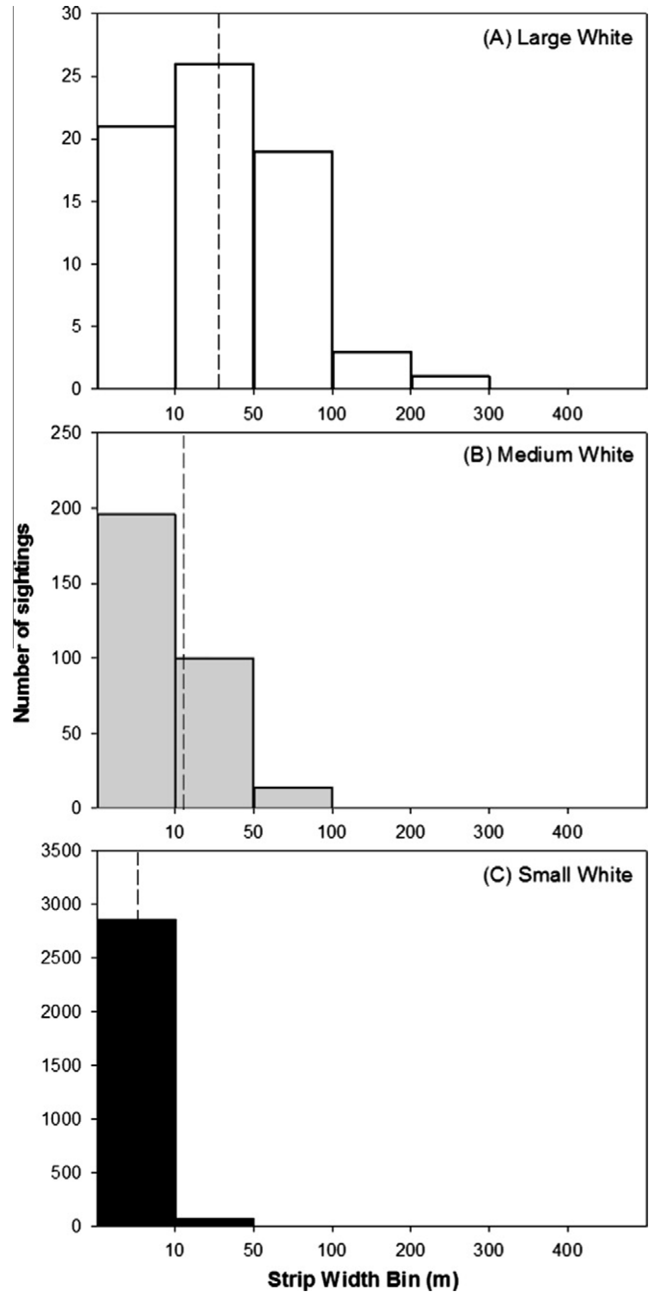

Fig. 5. Distribution of marine debris sightings based on the perpendicular distance from the vessel for large white pieces (A), medium white pieces (B) and small white pieces (C). The estimated strip width (ESW) is shown for each group (dashed line).

was sufficient to allow for all 3715 sightings to be included in the analysis. Conversely, we only considered those nine seabird species, which occurred in more than one survey day (Table 2) and included sightings of flying fish and flying squid in the analysis. After the removal of nine hourly transects due to their length, one seabird (Common Tern, *Sterna hirundo*) was only present during one day and so could not be included in the analysis (Table 2). All ten environmental and habitat variables were used as explanatory variables in the NMDS ordination, which produced a two axis solution that explained 80.2% of the observed variance in the concurrent bird and debris community composition. Axis one ($r^2 = 0.33$) captured a longitudinal gradient characterized by a decrease in temperature, depth and atmospheric pressure, and a concurrent increase in chlorophyll concentration (Table 7). Axis two ($r^2 = 0.47$) described a longitudinal gradient characterized by

Table 4
Results of the best-fit model parameters describing the perpendicular sighting distances used to estimate the effective strip width (ESW) for nine distinct marine debris groups based on size and color. The hazard rate (HR) or half normal (HN) models were chosen based on the minimum Akaike's Information Criteria (AIC).

MD group	Description	Sightings (sample size)	Model	Truncation (m)	$\alpha \pm$ SE	$\beta \pm$ SE	ESW ± SE (m)	AIC
1	Large white	70	HR	400	14.28 ± 6.49	1.33 ± 0.25	33.20 ± 8.58	193.92
2	Large high vis	32	HR	300	3.00 ± 3.52	1.59 ± 0.41	6.86 ± 5.66	62.31
3	Large low vis	83	HR	200	2.00 ± 3.47	1.37 ± 0.48	5.44 ± 6.19	145.95
4	Medium white	410	HR	100	7.67 ± 1.58	1.99 ± 0.24	13.02 ± 1.63	496.73
5	Medium high vis	72	HR	100	6.38 ± 3.24	2.15 ± 0.59	10.37 ± 3.36	102.08
6	Medium low vis	111	HR	100	3.96 ± 2.83	1.81 ± 0.44	7.48 ± 3.56	152.35
7	Small white	2925	HN	100	4.42 ± 0.88	–	5.54 ± 0.11	632.96
8	Small high vis	47	HN	100	6.59 ± 0.84	–	8.25 ± 1.05	37.90
9	Small low vis	62	HN	100	5.75 ± 0.65	–	7.20 ± 0.81	36.76

Table 5
Corrected number of sightings, encounter rate and density for each distinct marine debris group from the combined 74 hourly transects. The sighting data were corrected using the maximum ESW of 33.2 m (see Table 4).

MD group	Sightings	Correction factor	Corrected sightings	Corrected encounter rate (pieces km^{-1})	Corrected density (pieces km^{-2})
1	70	1.00	70.00	0.05	1.57
2	32	4.84	154.87	0.12	3.47
3	83	6.10	506.54	0.38	11.36
4	410	2.55	1045.47	0.78	23.44
5	72	3.20	230.51	0.17	5.17
6	111	4.44	492.67	0.37	11.04
7	2925	5.99	17,528.88	13.05	392.94
8	47	4.02	189.14	0.14	4.24
9	62	4.61	285.89	0.21	6.41

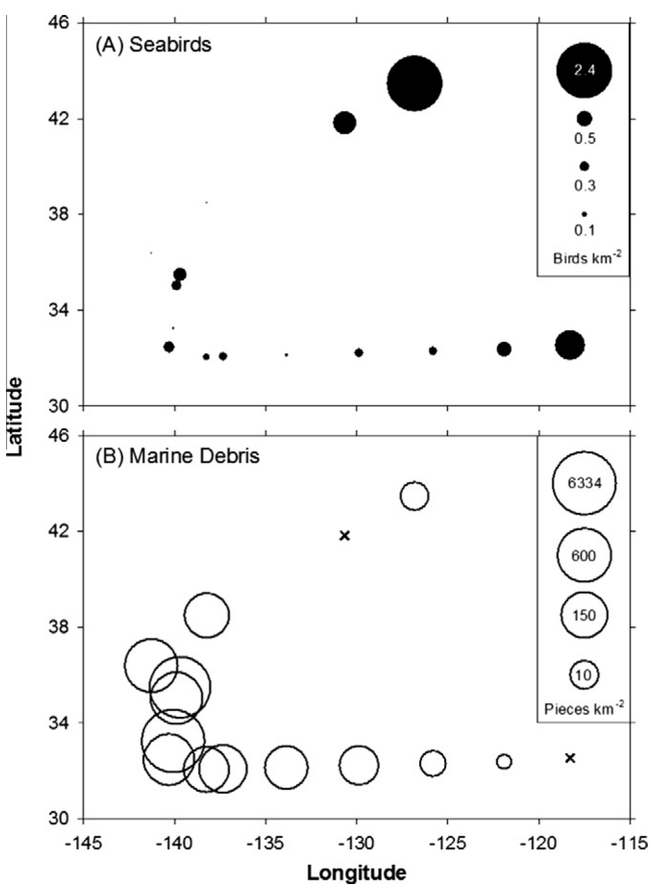

Fig. 6. Log-transformed densities of seabirds (A) and marine debris (B) within the study area. The circles are proportional to the densities at the midpoints of daily surveys, and × indicates absence (zero density).

an increase in temperature and depth, and a decrease in wind speed and chlorophyll concentration. These two axes were not perfectly orthogonal (76.3%), as evidenced by the shared influence of longitude, and were statistically significant ($p = 0.019$). Overall, the NMDS stress was 6.63, suggesting that it is a good ordination with no risk of drawing false inferences (Clarke, 1993).

The NMDS also revealed daily species-specific associations of the seabird taxa and marine debris groups. For instance, the daily samples were arranged into two clusters on the ordination plot: days 4–13 were characterized by deep subtropical gyre waters, and days 1, 2, 3, 14 and 15 were characterized by low atmospheric pressure and colder waters (Fig. 7A). The ordination plot of the species and marine debris groups closely resembled that of the daily surveys. The subtropical gyre samples supported the lowest bird densities and the highest debris densities. Furthermore, this cluster was characterized by the presence of all nine marine debris groups and tropical – sub-tropical avifauna (Black-footed Albatross BFAL; Cook's Petrel COPE, *Pterodroma cooki*; and Red-tailed Tropicbird RTTR), as well as Flying Fish (FF) and Flying Squid (FS). Conversely, the shallower, cold water samples were characterized by an avifauna dominated by transition zone and cosmopolitan taxa (Red-billed Tropicbird, RBTR, *Phaethon aethereus*; Leach's Storm-petrel LESP; Buller's Shearwater BUSH, *Puffinus bulleri*; and Ashy Storm-petrel ASSP, *Oceanodroma melania*). Two species, South-polar Skua (SPSK, *Catharacta maccormicki*) and Red-necked Phalarope (RNPH, *Phalaropus lobatus*) were not associated with either cluster due to their distribution across a wide range of environmental conditions (Fig. 7B). While the NMDS analysis of the daily surveys showed that three seabird species overlap with marine debris distributions at sea, the GLM analyses of the hourly transects showed that seabird and debris concentrations are spatially segregated (Fig. 6).

4. Discussion

This study quantified the concurrent community structure and distribution of marine debris and birds over a large area of the North East Pacific. Following the multi-scale approach advocated by Haury et al. (1978), our study documented different habitat associations of seabird and marine debris distributions over coarse-small meso scales (100s km) and small coarse scales (10s km). The large-scale analysis, using daily surveys, revealed

Table 6
Results of the step-wise multiple General Linear Model (GLM) analysis of marine debris density (A and B) and seabird density (C and D).

Variable	Coefficient	*t* Statistic	*p* Value	Result
(A) Marine debris location GLM, r^2 = 0.68, n = 74				
Latitude	−0.049	−2.622	0.011	Higher in South
Longitude	−0.132	−12.212	<0.001	Higher in West
(B) Marine debris environmental GLM of residuals, r^2 = 0.25, n = 74				
Wind speed	−0.206	−4.948	<0.001	Higher in low wind
Sea Level pressure	+0.062	+2.402	0.019	Higher in high pressure
Depth	+0.461	−3.649	0.001	Higher in deep water
(C) Seabird Location GLM, r^2 = 0.34, n = 74				
Latitude	+0.022	+5.001	<0.001	Higher in North
Longitude	+0.010	+3.950	<0.001	Higher in East
(D) Seabird Environmental GLM of residuals, r^2 = 0.11, n = 74				
Wind speed	−0.035	−3.253	0.002	Higher in low wind
Depth	−0.048	−2.412	0.018	Higher in shallow water

Table 7
Kendall tau correlation coefficients between the 10 environmental and habitat variables and the two non-metric multidimensional scaling (NMDS) axes used to characterize the concurrent distributions of seabirds and marine debris during 15 daily surveys.

Environmental variable	Axis 1	Axis 2
Wind speed (WSP)	−0.429	+0.295
Depth (DPT)	+0.600	−0.581
Temperature (SST)	+0.619	−0.752
CV temperature (TCV)	−0.410	+0.352
Chlorophyll-a concentration (CHL)	−0.067	+0.238
CV chlorophyll-a (CCV)	−0.524	+0.429
Sea level pressure (SLP)	+0.295	−0.505
Cloud cover (CC)	+0.010	+0.162
Latitude (LAT)	+0.162	+0.162
Longitude (LON)	−0.695	+0.524

that marine bird and debris communities were associated with specific water mass distributions (e.g., water temperature and productivity) and atmospheric patterns (e.g., sea-level pressure and wind). The small-scale analysis, using hourly transects, revealed distinct significant habitat associations of seabirds and marine debris suggestive of spatial segregation. Together, these results suggest that seabird and marine debris abundance and community structure in the North East Pacific are influenced by similar environmental processes (e.g., wind patterns and water masses), but in opposing ways, which leads to a spatial separation of the areas of high debris and seabirds aggregation (Figs. 6 and 7).

Our results showed that daily-scale marine debris distributions were related to two environmental factors, with denser concentration in oceanic (deep-water) and calm (higher atmospheric pressure, lower wind) areas. This conclusion agrees with previous studies of marine debris distributions in the North East Pacific from at-sea sampling (Day and Shaw, 1987; Moore et al., 2001) and oceanographic modeling (Kubota, 1994; Moore, 2003). These modeling results highlight debris retention at ocean convergence zones caused by surface Ekman drift along the subtropical North Pacific. Because Ekman drift and geostrophic currents are extremely weak within this zone of high atmospheric pressure zone, marine debris is effectively trapped and accumulated in this area (Kubota, 1994; Moore, 2003).

Additionally, the marine debris community showed some geographic and habitat separation between the nine groups we considered, with the smaller white pieces occurring furthest west in the area of the highest atmospheric pressure and warmest sea surface temperatures. This pattern suggests that the debris community within the center of the gyre is dominated by older (smaller and weathered) pieces, while a greater proportion of newer pieces

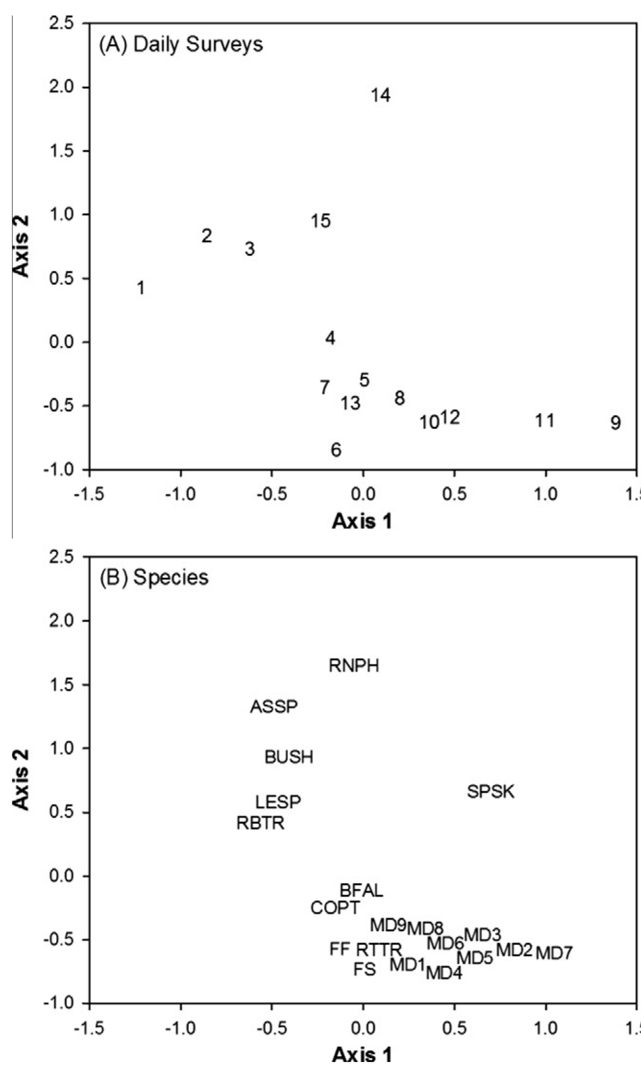

Fig. 7. Results of NMDS analysis of the concurrent seabird and debris community along 15 daily transects (A). Twenty species are plotted (B): the nine most common seabirds, the nine distinct debris groups, flying fish (FF) and flying squid (FS).

(larger and colorful) occur further towards the eastern edge of the large scale aggregation area. Notably, because the North American continent is located to the east of the study area, we hypothesize that this newer material likely originates from shore-based and river inputs.

While the community-level daily analysis documented large-scale marine debris concentration areas, the transect-level analysis did not identify specific habitat variables that explained the smaller-scale abundance of marine debris. The transect-level analysis documented higher marine debris abundance over deeper and warmer water and in areas of higher atmospheric pressure. However, when we tested for the influence of temperature and color fronts using fine-scale (resolution: 2-min, 0.6 km) sea surface temperature and chlorophyll-a concentration data collected by the vessel, we did not find any significant associations.

Nevertheless, the transect-scale analysis did reveal differences in marine debris and seabird abundance in relation to depth, with higher bird densities in shallower waters to the east. Higher summer-time seabird densities closer to shore are expected due to the central-place foraging distributions of breeding species and the higher productivity of continental shelf – slope waters (Gould and Piatt, 1993; Hyrenbach et al., 2007). As described previously, marine debris was more abundant in the deeper and lower productivity gyre waters to the west. This segregation of seabirds and debris by depth suggests that most seabirds were limited in their exposure to high concentrations of marine debris, although this was not the case for every species.

The community-level analysis, involving nine marine debris groups, nine seabird species and two seabird prey types, revealed that only a few trans-Pacific species overlapped with the large-scale area of high marine debris aggregation. Of the three species found to overlap with the debris, the Black-footed Albatross is highly susceptible to ingestion of marine debris (Blight and Burger, 1997; Kinan and Cousins, 2000) and the Cook's Petrel has a record of plastic ingestion during the breeding season (Imber, 1996). Yet, because both of these species are far-ranging surface foraging *procellariiform* seabirds, it is unclear when and where they collect this debris at sea. For instance, the albatross commute between their breeding colonies in Hawaii and specific foraging areas: the subtropical frontal system during the chick-brooding period (January–February) and the productive California Current System (CCS) during the chick-rearing period (March–June) (Hyrenbach et al., 2002; Kappes et al., 2010). The Cook's Petrel breeds in the southern hemisphere and migrates into the North Pacific during the austral winter and occur offshore of Mexico and California during April–November (Bartle et al., 1990), however, it was not one of the species studied for ingested plastic in the eastern topical Pacific by Spear et al. (1995). Thus, the high plastic aggregation zone we documented within the gyre is likely not an area of high foraging activity for these species, as evidenced by their low densities in this region (Wahl et al., 1989, this study). Nevertheless, because other oceanographic mechanisms, such as the Transition Zone Chlorophyll Front, aggregate marine debris across the North Pacific (Pichel et al., 2007) and provide persistent zones of enhanced convergence and localized productivity (Polovina et al., 2001), the far-ranging Black-footed Albatross and Cook's Petrel may be collecting the marine debris concentrated at these features.

Our estimates of marine debris densities from this visual survey are considerably lower than floating debris estimates derived from summer-time neuston net tows conducted in this area (Moore et al., 2001). For instance, our visual surveys revealed that debris densities varied widely but were significantly higher within the subtropical gyre, with the maximum estimated density during an hourly (16.8 km) transect of 15,222 pieces km^{-2}. In comparison, Moore et al. (2001) documented an average density of 334,271 pieces km^{-2} in this same area. Nevertheless, a critical distinction is that our visual survey samples a component of the debris field different from what is captured using neuston nets equipped with 333 micron-mesh. Although small (2–10 cm) pieces comprised the majority of the debris sighted in our study, we assumed that 2 cm was the lower end of detection, in agreement with the accepted lower range size for visual sampling (Ribic et al., 1992). Conversely, net tows target meso and micro debris (<2 cm), and rarely capture macro debris (>2 cm). This size segregation highlights the complementarity between visual and net tow surveys, and underscores the need to integrate both sampling methods to fully describe the debris field.

This study marks a step forward in quantifying mega and macro debris distributions at sea using rigorously-defined visual survey methods which do not require dedicated ship time and are easily transferable to other platforms. Line distance sampling techniques, which require no assumptions concerning the ability to visually detect marine debris of varying size and color, provide improved standardized abundance estimates based on empirically-derived observations. Furthermore, the analysis of different debris groups based on factors that affect their sightability (size and color) facilitates comparisons of the debris field composition over space and time. Our standardized approach does not require dedicated ship time and is easily transferable to any platform.

Our results highlighted patterns of marine debris distribution and abundance within the North East Pacific Ocean, and documented large-scale (day, 100s km) aggregations associated with the subtropical gyre (an area of higher sea surface temperature and atmospheric pressure), and small-scale (transect, 10s km) variability within this aggregation area. Furthermore, our results showed that only two far ranging petrels overlap with this zone of debris aggregation in the North East Pacific.

These coarse-scale (10s km) aggregations of seabirds and marine debris are difficult to characterize, and are likely influenced by dynamic physical processes (e.g., convergence zones that aggregate floating material and make seabird prey available, Franks, 1992; Hyrenbach et al., 2006) and by short-lived physical and biological processes (e.g., seabird interactions with subsurface-predators, prey; Pitman and Ballance, 1990; Hebshi et al., 2008). Thus, a better understanding of these small-scale patterns of habitat use and aggregation appear critical to identify those locations where seabirds are at risk from plastic ingestion at-sea.

Acknowledgements

We wish to thank the captain and crew of the *R/V New Horizon* and the Scripps Institution of Oceanography for their support and expertise at sea. This research could not have been possible without the invitation from Miriam Goldstein, and from the SEAPLEX SEAPLEX program, funded by University of California Ship Funds, Project Kaisei/Ocean Voyages Institute, and NSF IGERT (Grant 0333444). NOAA and the National Fish and Wildlife Foundation Marine Debris Programs (Grant 2007-0088-007 to KDH) funded this research.

References

Amante, C., Eakins, B.W., 2009. ETOPO1 1 arc-minute global relief model: Procedures, data sources and analysis. NOAA technical memorandum NESDIS NGDC-24, 19pp, March 2009.

Andrady, A.L., 2005. Plastics in the marine environment, a technical perspective. In: Proceedings of the Plastic Debris Rivers to Sea Conference, 2005. Algalita Marine Research Foundation, Long Beach, CA.

Ballance, L.T., Pitman, R.L., 1998. Cetaceans of the western tropical Indian Ocean: distribution relative abundance, and comparisons with cetacean communities of two other tropical ecosystems. Marine Mammal Science 14, 429–459.

Barnes, D.K.A., Galgani, F., Thompson, R.C., Barlaz, M., 2009. Accumulation and fragmentation of plastic debris in global environments. Philosophical Transactions of the Royal Society B 364, 1985–1998.

Bartle, J.A., Hu, D., Stahl, J.C., Pyle, P., Simons, T.R., Woodby, D., 1990. Status and ecology of gadfly petrels in the temperate North Pacific. In: Vermeer, K., Briggs, K.T., Morgan, K.H., Siegel-Causey, D. (Eds.), The status, ecology, and conservation of marine birds of the North Pacific. Canadian Wildlife Service Special Publication, Ottawa, pp. 101–111.

Blight, L.K., Burger, A.E., 1997. Occurrence of plastic particles in sea-birds from the eastern North Pacific. Marine Pollution Bulletin 34, 323–325.

Boerger, C.M., Lattin, G.L., Moore, S.L., Moore, C.J., 2010. Plastic ingestion by planktivorous fishes in the North Pacific Central Gyre 60, 2275–2278.
Buckland, S.T., Anderson, D.R., Burnham, K.P., Laake, J.L., 1993. Distance Sampling: Estimating Abundance of Biological Populations. Chapman & Hall, London.
Chai, F., Jiang, M., Barber, R.T., Dugdale, R.C., Chao, Y., 2003. Interdecadal variation of the Transition Zone Chlorophyll Front, a physical–biological model simulation between 1960 and 1990. Journal of Oceanography 59, 461–475.
Clarke, K.R., 1993. Non-parametric multivariate analyses of changes in community structure. Australian Journal of Ecology 18, 117–143.
Dahlberg, M.L., Day, R.H., 1985. Observations of man-made objects on the surface of the North Pacific Ocean. In: Shomura, R.S., Yoshida, H.O. (Eds.), Proceedings of the Workshop on the Fate and Impact of Marine Debris, 26–29 November 1984. Honolulu, Hawaii.
Day, R.H., Shaw, D.G., 1987. Patterns in the abundance of pelagic plastic and tar in the North Pacific Ocean, 1976–1985. Marine Pollution Bulletin 18, 311–316.
Derraik, J.G.B., 2002. The pollution of the marine environment by plastic debris: a review. Marine Pollution Bulletin 44, 842–852.
Fauchald, P., Erikstad, K.E., Skarsfjord, H., 2000. Scale-dependent predator-prey interactions: the hierarchical spatial distribution of seabirds and prey. Ecology 81, 773–783.
Forney, K.A., Barlow, J., 1993. Preliminary winter abundance estimates for cetaceans along the California coast based on a 1991 aerial survey. Reports of the International Whaling Commission 43, 407–415.
Franks, P.J.S., 1992. Sink or swim: accumulation of biomass at fronts. Marine Ecology-Progress Series 82, 1–12.
Gould, P.J., Piatt, J.F., 1993. Seabirds of the central North Pacific. In: Vermeer, K., Briggs, K.T., Morgan, K.H., Siegel-Causey, D. (Eds.), The Status, Ecology, and Conservation of Marine Birds in the North Pacific. Canadian Wildlife Service Special Publication, Ottawa, pp. 27–38.
Haury, L.R., McGowan, J.A., Wiebe, P.H., 1978. Patterns and processes in the time-space scales of plankton distribution. In: Steele, J.H. (Ed.), Spatial Pattern in Plankton Communities. Plenum, New York, pp. 277–327.
Hebshi, A.J., Duffy, D.C., Hyrenbach, K.D., 2008. Associations between seabirds and subsurface predators around Oahu, Hawaii. Aquatic Biology 4, 89–98.
Heinemann, D., 1981. A range-finder for pelagic bird censusing. Journal of Wildlife Management 45, 489–493.
Hunt Jr., G.L., Mehlum, F., Russell, R.W., Irons, D., Decker, M.B., Becker, P.H., 1999. Physical processes, prey abundance, and the foraging ecology of seabirds. In: Adams, N.J., Slotow, R.H., (Eds.), Proceedings of the 22nd International Ornithological Congress. Durban, Bird Life South Africa, Johannesburg, pp. 2040–2056.
Hyrenbach, K.D., Baduini, C.L., Hunt Jr., G.L., 2001. Line transect estimates of Short-tailed Shearwater *Puffinus tenuirostris* mortality in the South-Eastern Bering Sea, 1997–1999. Marine Ornithology 29, 11–18.
Hyrenbach, K.D., Fernández, P., Anderson, D.J., 2002. Oceanographic habitats of two sympatric North Pacific albatrosses during the breeding season. Marine Ecology Progress Series 233, 283–301.
Hyrenbach, K.D., Viet, R.R., Weimerskirch, H., Hunt Jr., G.L., 2006. Seabird associations with mesoscale eddies: the subtropical Indian Ocean. Marine Ecology Progress Series 342, 271–279.
Hyrenbach, K.D., Henry, M.F., Morgan, K.H., Welch, D.W., Sydeman, W.J., 2007. Optimizing the widths of strip transects for seabird surveys from vessels of opportunity. Marine Ornithology 35, 29–38.
Imber, M.J., 1996. The food of Cook's Petrel *Pterodroma cooki* during its breeding season on Little Barrier Island, New Zealand. Emu 96, 189–194.
Kappes, M.A., Shaffer, S.A., Tremblay, Y., Foley, D.G., Palacios, D.M., Robinson, P.W., Bograd, S.J., Costa, D.P., 2010. Hawaiian albatrosses track interannual variability of marine habitats in the North Pacific. Progress in Oceanography 86, 246–260.
Kinan, I.T., Cousins, K.L., 2000. Abundance of plastic debris and ingestion by albatross on Kure Atoll, Northwestern Hawaiian Islands. In: Second International Conference on the Biology and Conservation of Albatrosses and other Petrels, 8–10 May 2000. Waikiki, Hawaii.
Kubota, M., 1994. A mechanism for the accumulation of floating marine debris north of Hawaii. Journal of Physical Oceanography 24, 1059–1064.
Laist, D.W., 1987. Overview of the biological effects of lost and discarded plastic debris in the marine-environment. Marine Pollution Bulletin 18, 319–326.
Laist, D.W., 1997. Impacts of marine debris: entanglement of marine life in marine debris including a comprehensive list of species with entanglement and ingestion records. In: Coe, J.M., Rogers, D.B. (Eds.), Marine Debris: Sources, Impacts and Solutions. Springer Series on Environmental Management. pp. 99–139.
Law, K.L., Morét-Ferguson, S., Maximenko, N.A., Proskurowski, G., Peacock, E.E., Hafner, J., Reddy, C.M., 2010. Plastic accumulation in the North Atlantic Subtropical Gyre. Science 329, 1185–1188.
Mallory, M.L., 2008. Marine plastic debris in Northern Fulmars from the Canadian high Arctic. Marine Pollution Bulletin 56, 1501–1504.
McCune, B., Mefford, M.J., 1999. PC-ORD: Multivariate Analysis of Ecological Data (Version 4). MjM Software Design, Gleneden Beach, OR.
Moore, C.J., 2003. Trashed: across the Pacific Ocean plastics, plastics everywhere. Natural History 112, 46–51.
Moore, C.J., 2008. Synthetic polymers in the marine environment: a rapidly increasing, long-term threat. Environmental Research 108, 131–139.
Moore, C.J., Moore, S.L., Leecaster, M.K., Weisberg, S.B., 2001. A comparison of plastic and plankton in the North Pacific central gyre. Marine Pollution Bulletin 42, 1297–1300.
Morét-Ferguson, S., Law, K.L., Proskurowski, G., Murphy, E.K., Peacock, E.E., Reddy, C.M., 2010. The size, mass, and composition of plastic debris in the western North Atlantic Ocean. Marine Pollution Bulletin 60, 1873–1878.
Nevins, H., Hyrenbach, K.D., Keiper, C., Stock, J., Hester, M., Harvey, J., 2005. Seabirds as indicators of plastic pollution in the North Pacific. Plastic Debris Rivers to the Sea, Redondo Beach, CA. http://conference.plasticdebris.org/whitepapers.shtml.
Pichel, W.G., Churnside, J.H., Veenstra, T.S., Foley, D.G., Friedman, K.S., Brainard, R.E., Nicoll, J.B., Zheng, Q., Clemente-Colon, P., 2007. Marine debris collects within the North Pacific Subtropical Convergence Zone. Marine Pollution Bulletin 54, 1207–1211.
Pitman, R.L., Ballance, L.T., 1990. Daytime feeding by Leach's Storm-petrel on a midwater fish in the eastern tropical Pacific. Condor 92, 524–527.
Polovina, J.J., Howell, E., Kobayashi, D.R., Seki, M.P., 2001. The Transition Zone Chlorophyll Front, a dynamic global feature defining migration and forage habitat for marine resources. Progress in Oceanography 49, 469–483.
Ribic, C.A., Dixon, T.R., Vining, I., 1992. Marine debris survey manual. NOAA Technical Report NMFS 108.
Robards, M.D., Piatt, J.F., Wohl, K.D., 1995. Increasing frequency of plastic particles ingested by seabirds in the sub-arctic North Pacific. Marine Pollution Bulletin 30, 151–157.
Robards, M.D., Gould, P.J., Piatt, J.F., 1997. The highest global concentrations and increased abundance of oceanic plastic debris in the North Pacific: evidence from seabirds. In: Coe, J.M., Rogers, D.B. (Eds.), Marine Debris: Sources, Impacts and Solutions. Springer, New York, pp. 71–80.
Ronconi, R.A., Burger, A.E., 2009. Estimating seabird densities from vessel transects: distance sampling and implications for strip transects. Aquatic Biology 4, 297–309.
Ryan, P.G., Fraser, M.W., 1988. The use of Great Skua pellets as indicators of plastic pollution in seabirds. Emu 88, 16–19.
Ryan, P.G., Moore, C.J., van Franeker, J.A., Moloney, C.L., 2009. Monitoring the abundance of plastic debris in the marine environment. Philosophical Transactions of the Royal Society B 364, 1999–2012.
Sileo, L., Sievert, P.R., Samuel, M.D., Fefer, S.I., 1990. Prevalence and characteristics of plastic ingested by Hawaiian seabirds. In: Shomura, R.S., Godfrey, M.L., (Eds.). Proceedings of the Second International Conference on Marine Debris, 2–7 April 1989, Honolulu, Hawaii. US Dept. Commer., NOAA Tech. Memo. NMFS, NOAA-TM-NMFS-SWFSC-154.
Spear, L.B., Ainley, D.G., Ribic, C.A., 1995. Incidence of plastic in seabirds from the tropical Pacific, 1984–91 – Relation with distribution of species, sex, age, season, year and body-weight. Marine Environmental Research 40, 123–146.
Tasker, M.L., Hope Jones, P., Dixon, T., Blake, B.F., 1984. Counting seabirds from ships: a review of methods employed and a suggestion for a standardized approach. Auk 101, 567–577.
Thomas, L., Buckland, S.T., Rexstad, E.A., Laake, J.L., Strindberg, S., Hedley, S.L., Bishop, J.R.B., Marques, T.A., Burnham, K.P., 2010. Distance software: design and analysis of distance sampling surveys for estimating population size. Journal of Applied Ecology 47, 5–14.
UNEP, 2005. Marine Litter, An Analytical Overview.
Wahl, T.R., Ainley, D.G., Benedict, A.H., DeGange, A.R., 1989. Associations between seabirds and water-masses in the northern Pacific Ocean in summer. Marine Biology 103, 1–11.
Young, L.C., Vanderlip, C., Duffy, D.C., Afanasyev, V., Shaffer, S.A., 2009. Bringing home the trash: do colony based differences in foraging distribution lead to increased plastic ingestion in Laysan albatrosses? PLoS ONE 4 (10), e7623.
Zar, J.H., 1984. Biostatistical Analysis. Prentice-Hall, Englewood Cliffs, NJ.